

## PLATELETS AND THROMBOPOIESIS

## Pak2 restrains endomitosis during megakaryopoiesis and alters cytoskeleton organization

Rachelle E. Kosoff,<sup>1,2</sup> Joseph E. Aslan,<sup>3</sup> John C. Kostyak,<sup>4</sup> Essel Dulaimi,<sup>5</sup> Hoi Yee Chow,<sup>1</sup> Tatiana Y. Prudnikova,<sup>1</sup> Maria Radu,<sup>1</sup> Satya P. Kunapuli,<sup>4</sup> Owen J. T. McCarty,<sup>3</sup> and Jonathan Chernoff<sup>1</sup>

<sup>1</sup>Cancer Biology Program, Fox Chase Cancer Center, Philadelphia, PA; <sup>2</sup>Cell and Molecular Biology, University of Pennsylvania School of Medicine, Philadelphia, PA; <sup>3</sup>Department of Biomedical Engineering, Oregon Health and Science University, Portland, OR; <sup>4</sup>Sol Sherry Thrombosis Research Center, Department of Pharmacology, Temple University School of Medicine, Philadelphia, PA; and <sup>5</sup>Department of Pathology, Fox Chase Cancer Center, Philadelphia, PA

## Key Points

- Bone marrow-specific deletion of *Pak2* is associated with macrothrombocytopenia and abnormal megakaryocyte morphology and function.
- *Pak2* deletion is associated with defects in megakaryocyte endomitosis and the activation of Aurora-A and LIM kinase.

Megakaryocyte maturation and polyploidization are critical for platelet production; abnormalities in these processes are associated with myeloproliferative disorders, including thrombocytopenia. Megakaryocyte maturation signals through cascades that involve p21-activated kinase (Pak) function; however, the specific role for Pak kinases in megakaryocyte biology remains elusive. Here, we identify Pak2 as an essential effector of megakaryocyte maturation, polyploidization, and proplatelet formation. Genetic deletion of *Pak2* in murine bone marrow is associated with macrothrombocytopenia, altered megakaryocyte ultrastructure, increased bone marrow megakaryocyte precursors, and an elevation of mature CD41<sup>+</sup> megakaryocytes, as well as an increased number of polyploid cells. In *Pak2*<sup>-/-</sup> mice, platelet clearance rate was increased, as was production of newly synthesized, reticulated platelets. In vitro, *Pak2*<sup>-/-</sup> megakaryocytes demonstrate increased polyploidization associated with alterations in  $\beta$ 1-tubulin expression and organization, decreased proplatelet extensions, and reduced phosphorylation of the en-

domitosis regulators LIM domain kinase 1, cofilin, and Aurora A/B/C. Together, these data establish a novel role for Pak2 as an important regulator of megakaryopoiesis, polyploidization, and cytoskeletal dynamics in developing megakaryocytes. (*Blood*. 2015;125(19):2995-3005)

## Introduction

Megakaryocytes are both the largest (50-100  $\mu$ m) and rarest (~0.03%-0.06%) cell type in the bone marrow.<sup>1,2</sup> To produce sufficient numbers of platelets, these cells become polyploid and undergo massive nuclear proliferation, together with an enlargement of the megakaryocyte cytoplasm, which becomes filled with platelet-specific granules. Megakaryocytes undergo a complex maturation process by which their cytoplasmic contents are packaged into multiple elongated proplatelet processes.<sup>3</sup> As proplatelets extend through the sinusoid vessels, physiological shear force aids in dissociating proplatelets into circulating platelets.<sup>4,5</sup> Megakaryocyte maturation is triggered primarily through cellular signaling events initiated by the cytokine thrombopoietin (TPO).<sup>6</sup> TPO binds to the c-Mpl receptor on megakaryocytes to activate the Janus kinase-2 signaling pathway and stimulates the phosphatidylinositol 3 kinase (PI3K)/Akt and mitogen-activated protein kinase pathways.<sup>7-9</sup>

The p21-activated kinases (Paks) are serine/threonine kinases that support cell homeostasis, contractility, and survival processes.<sup>10</sup> After their activation by the  $\rho$  GTPases, Rac1 and Cdc42, Paks phosphorylate dozens of effector proteins to regulate the mitogen-activated protein kinase signaling and cytoskeletal remodeling.<sup>11-14</sup> Accordingly, the Paks regulate numerous hematopoietic processes, including hematopoietic stem cell engraftment and homing to the

bone marrow, assembly of the actin cytoskeleton, and chemotaxis.<sup>15</sup> In addition, Paks promote hematopoiesis by regulating Raf-1 and Mek-1 activation to drive Erk1/2 activation, resulting in proper hematopoietic function.<sup>16</sup> Paks also have roles in platelet activation through the orchestration of platelet signaling and cytoskeletal dynamics.<sup>17-24</sup> Moreover, mice with megakaryocyte-specific double-knockout deletions of the Pak-activating proteins, Rac1/Cdc42, develop abnormal megakaryocyte morphologies, which fail to form proplatelets, resulting in macrothrombocytopenia.<sup>25</sup> Although Pak activation is compromised in megakaryocyte and platelet systems lacking Cdc42 and Rac1, a specific role for Paks in megakaryocyte development and function has yet to be defined.<sup>23-25</sup>

Here, we sought to determine the contribution of group I Paks (Pak 1-3) to the process of megakaryocyte maturation. We found that bone marrow-specific deletion of *Pak2* is associated with macrothrombocytopenia and decreased platelet half-life, together with increased megakaryocyte ploidy and altered microfilament and microtubule proplatelet structures. These effects are accompanied by defective activation of the Pak substrates, LIM domain kinase 1 (LIMK) and Aurora, in megakaryocytes. Together, our findings suggest a novel function for *Pak2* in megakaryocyte development and warrant consideration as small-molecule inhibitors of Paks are developed as clinical agents.<sup>26-30</sup>

Submitted October 8, 2014; accepted March 17, 2015. Prepublished online as *Blood* First Edition paper, March 30, 2015; DOI 10.1182/blood-2014-10-604504.

The online version of this article contains a data supplement.

The publication costs of this article were defrayed in part by page charge payment. Therefore, and solely to indicate this fact, this article is hereby marked "advertisement" in accordance with 18 USC section 1734.

© 2015 by The American Society of Hematology

## Materials and methods

### Generation of mice with *Pak2*<sup>-/-</sup> bone marrow

*Pak2*-deficient mice were generated by crossing *Pak2*-floxed mice with mice carrying the *Mx1-cre* transgene (M.R. and J.C., manuscript in preparation).<sup>15,31,32</sup> In 3-month-old mice, wild-type and *Mx1-cre*<sup>+</sup>*Pak2*<sup>fl/fl</sup> mice were injected with 400 μg polyinosinic:polycytidylic acid (pIpC) every other day. Fourteen days after the first injection, mice were euthanized for experiments.

### Administration of drug treatment

Animals received vehicle or Frax 1036 (30 mg/kg) via daily oral gavage, diluted in 20% (2-hydroxypropyl)-β-cyclodextrin (Sigma-Aldrich) for 3 weeks, according to a previously published protocol.<sup>33</sup> Severe combined immunodeficiency animals were used for drug treatment, as C57BL/6 animals were hypersensitive to drug treatment. All animal studies were performed according to protocols approved by the Fox Chase Cancer Center Institutional Animal Care and Use Committee.

### Antibodies and reagents

All reagents were purchased from Sigma-Aldrich unless otherwise stated. Antibodies for western blotting (WB) against pLIMK (T508), pCofilin (S3), and pAurora A/B/C (T288/T232/T198) and total protein (LIMK, cofilin) were from Cell Signaling. Anti-Aurora A was from BD Biosciences. WB technique on day 5 megakaryocytes was carried out as previously described by our laboratory.<sup>13</sup> Recombinant mouse TPO was from Shenandoah Biotechnology. Interleukin 3 (IL-3) and IL-6 were purchased from PeproTech. Antibodies for fluorescence-activated cell sorting were from Ebioscience (antibody name [clone] murine hematopoietic lineage eFluor 450 cocktail, c-Kit-APC (2B8), sca-1-phycoerythrin (PE)-Cy7 (D7), CD150-FITC (BioLegend-TC15-12F12.2), CD41-APC-Cy7 and CD41-eFluor 450 (MWRReg30), CD105-PE (MJ7/18), and FcγII/III-PerCP-eFluor 710(clone 93). Antibodies for immunofluorescence (CD41 and β1-tubulin) were from Abcam. Frax 1036 was kindly supplied by Genentech.

### Analysis of platelet clearance and production

To determine platelet clearance, an *in vivo* biotinylation approach was used.<sup>34</sup> Briefly, 10 days after pIpC, mice were IV injected with sulfo-*N*-hydroxysulfosuccinimidobiotin-biotin (Pierce Chemical). After blood collection daily with retroorbital bleeds, the blood was diluted in phosphate-buffered saline and incubated with streptavidin-PE (BD Biosciences) to label biotinylated platelets. Thiazole orange (10 μg/mL) was then added to measure reticulated platelets, after which samples were fixed in 1% formalin and analyzed on an LSR-II (BD Biosciences).

### Bone marrow collection and MegaCult-C assays

Bone marrow cell suspension was isolated from the tibias and femurs of pIpC-treated mice. Bone marrow was flushed and filtered through a 100-μm nylon strainer, followed by red blood cell lysis and antibody staining. For MegaCult-C assays, a total of 10<sup>5</sup> unsorted bone marrow cells were seeded, according to the manufacturer's protocols (Stem-Cell Technologies), and cultured with 50 ng/mL TPO, 10 ng/mL IL-3, and 10 ng/mL IL-6. Cultures were incubated for 10 days and then fixed and stained for acetylcholinesterase according to the manufacturer's protocol.

### Measurement of hematological parameters

Mice were euthanized with CO<sub>2</sub>, and blood was extracted via the hepatoportal vein with a syringe containing acid-citrate dextrose (10% final) and added into EDTA tubes. Counts were performed using a VetScan HM5 (Abaxis).

### In vitro culture of bone marrow-derived megakaryocytes

*In vitro* assays used *CAGG-Cre-ERT2*<sup>+</sup>*Pak2*<sup>fl/fl</sup> bone marrow, with deletion of *Pak2* induced with 500 nM 4-hydroxytamoxifen. Frax 1036 treatment of cultured megakaryocytes was performed at a concentration of 1 μM. Bone marrow-megakaryocytes were cultured for 5 days in Dulbecco's modified Eagle medium,

10% fetal bovine serum, penicillin/streptomycin, and 75 ng/mL TPO and fractionated on a 1.5%/3% discontinuous bovine serum albumin gradient.

### Megakaryocyte ploidy analysis

For ploidy measurements, cells were analyzed as described previously.<sup>35</sup> DNA content in CD41<sup>+</sup> megakaryocytes was determined by labeling red blood cell-lysed bone marrow with anti-CD41-eFluor450, followed by fixation with 0.5% formalin. Cells were permeabilized with 70% ice-cold methanol and washed and incubated with 10 μg RNase A, followed by brief incubation with 1 μg/μL propidium iodide. Cells were analyzed on an LSR-II.

### Proplatelet analysis

Bone marrow-derived megakaryocytes on day 5 were added to fibrinogen-coated plates and imaged at 5 and 24 hours. The amount of proplatelet extensions, relative to total megakaryocytes, was enumerated by light microscopy (×20 objective, EVOS, Invitrogen). At least 10 images per genotype (*n* > 5/genotype) were used to evaluate the number of proplatelet-forming megakaryocytes.

### Analysis of megakaryocyte progenitor cells

To analyze megakaryocyte stem cells, the protocol from Pronk et al was followed.<sup>36</sup> Bipotential megakaryocyte/erythroid progenitor (PreMegE) cells were gated as lin<sup>-</sup>sca1<sup>-</sup>ckit<sup>+</sup>CD41<sup>-</sup>FcγII/III<sup>-</sup>CD105<sup>-</sup>CD150<sup>+</sup>, and megakaryocyte progenitors were gated as lin<sup>-</sup>sca1<sup>-</sup>ckit<sup>+</sup>CD150<sup>+</sup>CD41<sup>+</sup>.<sup>36</sup> Megakaryocytes were analyzed by anti-CD41-APC-Cy7 and calculated as percentage of total bone marrow. Flow cytometric data collection was performed on an LSRII and analyzed with FlowJo software (TreeStar).

### Immunofluorescence microscopy

*In vitro* bone marrow-derived megakaryocytes adhered to fibrinogen-coated slides (200 ng/mL) for 5 hours in the presence of TPO. Cells were fixed with 2% paraformaldehyde and centrifuged onto coated slides for 5 minutes at 1000 *g*. Cells were permeabilized with 0.5% triton X-100 for 5 minutes before blocking for 1 hour and antibody incubation overnight. Slides were counterstained with 4',6-diamidino-2-phenylindole (DAPI) and phalloidin and were mounted in ProLong gold before visualization. Confocal microscopy was done on an inverted Leica SP8 3 channel confocal system at ×63 magnification. Image analysis was performed with Fiji software (National Institutes of Health).

### Histology

Five-μm sections of paraffin-embedded sternum and spleen were stained with hematoxylin and eosin and analyzed for megakaryocytes using an Olympus BX53 microscope (×40 objective).

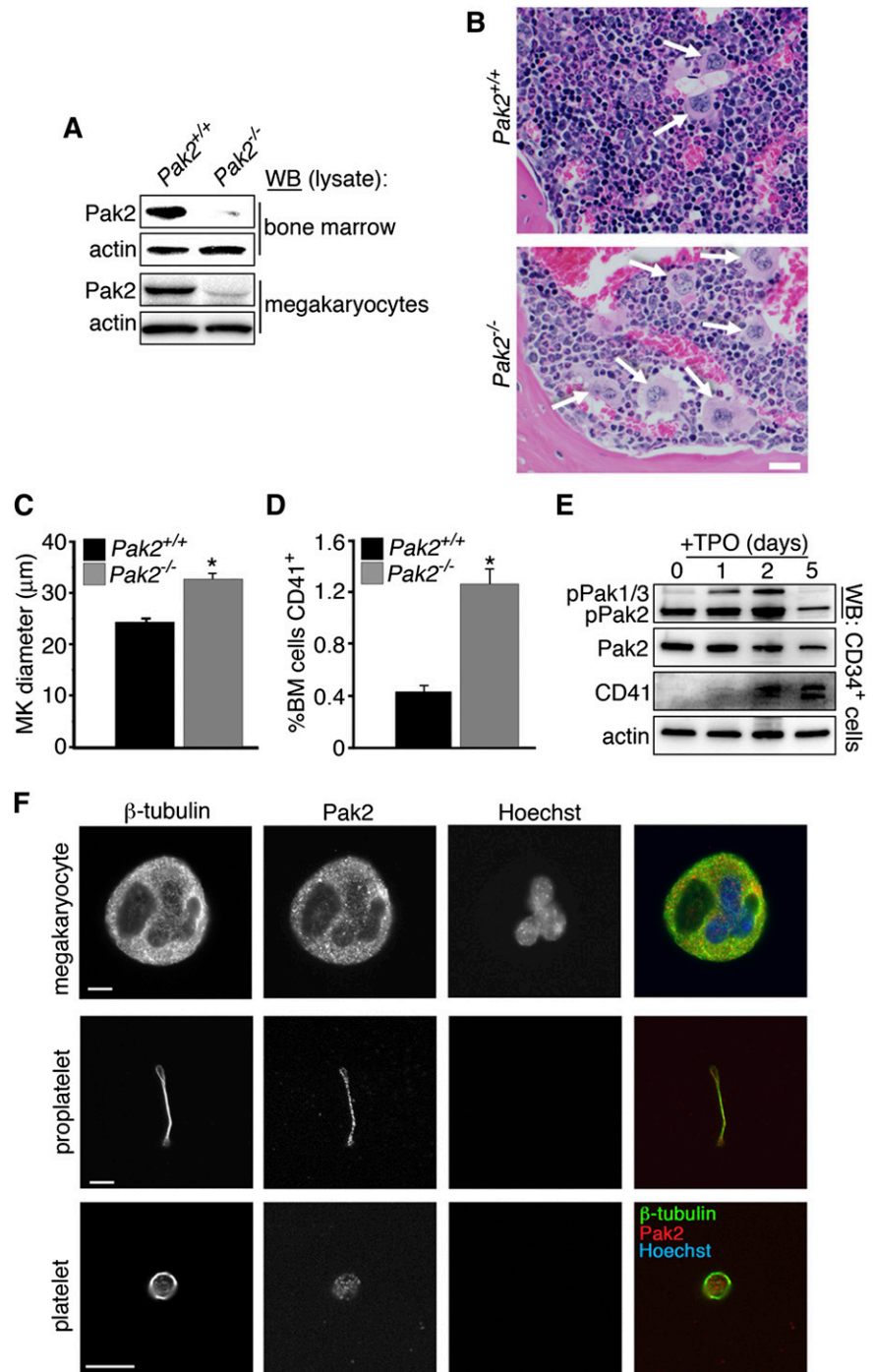
### Transmission electron microscopy

Bone marrow cores from mice 14 days post-pIpC were fixed with 2.5% glutaraldehyde, 2.0% paraformaldehyde in 0.1 M sodium cacodylate buffer at pH 7.4 for 24 hours at 4°C. After subsequent buffer washes, the samples were postfixed in 2.0% osmium tetroxide for 1 hour at room temperature, washed, and placed in dH<sub>2</sub>O. After dehydration through a graded ethanol series, bone marrow was infiltrated and embedded in EMbed-812 (Electron Microscopy Sciences). Thin sections were stained with uranyl acetate and lead citrate and examined with a JEOL 1010 electron microscope fitted with a Hamamatsu digital camera and AMT Advantage image capture software.

### Statistical analysis

The data presented in this report are the result of at least 3 independent experiments with individual mice per genotype. Statistical analysis was performed using a 2-tailed Student *t* test, and a *P* value < .05 was considered statistically significant.

**Figure 1. *Pak2* deletion stimulates megakaryopoiesis in vivo.** (A) WB to detect *Pak2* levels in bone marrow (top) and megakaryocytes (bottom) 14 DPI. Actin serves as a loading control for relative protein levels. Megakaryocytes lysates collected from cultured bone marrow of plpC-injected *Mx1-cre<sup>+</sup>;Pak2<sup>fl/fl</sup>* and wild-type (notated as *Pak2<sup>-/-</sup>* and *Pak2<sup>+/+</sup>*, respectively) mice at 14 DPI. (B) Representative bone marrow histology from *Pak2<sup>+/+</sup>* and *Pak2<sup>-/-</sup>* mice (n = 5 mice/genotype), both treated with plpC and analyzed 14 DPI. White arrows indicate megakaryocytes. Scale bar = 20  $\mu$ m ( $\times$ 40 original magnification). (C) Measurement of megakaryocyte diameter in the bone marrow (n = 5 mice/genotype). (D) Percentage of bone marrow expressing CD41 measured by flow cytometry. (E) CD34<sup>+</sup> bone marrow stem cells sorted by flow cytometry and cultured with 100 ng/mL TPO for 5 days. Representative WB of phospho-Pak1/2/3 (Serine141) and *Pak2* expression during a 5-day time course. Actin serves as a loading control for total protein levels. CD41 expression marks mature megakaryocytes. (F) Fluorescence microscopy of megakaryocyte (top), proplatelet (middle), and platelet (bottom) stained for  $\beta$ 1-tubulin, *Pak2*, and nuclei (Hoechst). Scale bar = 10  $\mu$ m. All values are mean  $\pm$  standard error of the mean (SEM) for at least 5 mice/genotype. \**P* < .05.



## Results

### Inducible deletion of *Pak2* results in macrothrombocytopenia in adult mice

To study the function of the *Pak2* gene in various hematopoietic-derived cells, mice carrying conditional *Pak2<sup>fl/fl</sup>* alleles were crossed with mice harboring the interferon-inducible Mx1-Cre transgene to produce *Mx1<sup>tg</sup>;Pak2<sup>fl/fl</sup>* (*Pak2<sup>-/-</sup>*) and *Mx1<sup>tg</sup>;Pak2<sup>+/+</sup>* controls (wild-type) (M.R. and J.C., manuscript in preparation).<sup>31</sup> Deletion of the floxed exon 2, which encodes the start site of *Pak2*, was achieved by

intraperitoneal administration of plpC. Neither *Pak2* protein levels in the bone marrow nor megakaryocytes were detectable 14 days post-plpC (DPI) (Figure 1A). Deletion in megakaryocytes of *Pak2<sup>-/-</sup>* mice was confirmed by culturing bone marrow extracted at 14 DPI with TPO for 5 days.

Complete blood count analysis of *Pak2<sup>-/-</sup>* and wild-type mice displayed moderate thrombocytopenia (wild-type,  $997 \times 10^3/\mu\text{L}$  [ $\pm 98 \times 10^3$ ], n = 29; *Pak2<sup>-/-</sup>*,  $498 \times 10^3/\mu\text{L}$  [ $\pm 25 \times 10^3$ ], n = 52; Table 1). Platelet size was significantly increased, as determined by mean platelet volume (MPV; wild-type,  $6.56 \pm 0.05$  fL vs *Pak2<sup>-/-</sup>*  $7.1 \pm 0.07$  fL, *P* < .001). Additional changes in blood counts included

**Table 1. Complete blood count profile for Pak2-deficient mice**

Parameters	Mx1Cre <sup>Tg</sup> Pak2 <sup>+/+</sup>	Mx1Cre <sup>Tg</sup> Pak2 <sup>fl/fl</sup>
White blood cells, ×10 <sup>3</sup> /μL	8.97 ± 0.44	7.6 ± 0.4
Neutrophils, ×10 <sup>3</sup> /μL	0.97 ± 0.1	2.3 ± 0.13*
Lymphocytes, ×10 <sup>3</sup> /μL	7.5 ± 0.3	5.4 ± 0.3
Monocytes, ×10 <sup>3</sup> /μL	0.16 ± 0.01	0.25 ± 0.02
Red blood cells, ×10 <sup>12</sup> /L	9.87 ± 0.27	9.67 ± 0.25
Hemoglobin, g/L	14.43 ± 0.42	14.57 ± 0.29
HCT, %	44.9 ± 1.3	45.73 ± 0.85
MCV, fL	44.37 ± 1.12	46.09 ± 0.39
Platelets, ×10 <sup>9</sup> /L	997 ± 98	498 ± 25*
MPV, fL	6.56 ± 0.05	7.1 ± 0.07*

HCT, hematocrit; MCV, mean corpuscular volume; MPV, mean platelet volume.  
\**P* < .05

increased neutrophils and monocytes and decreased lymphocytes (Table 1). Deletion of *Pak1* did not affect peripheral blood indices, including no changes in platelet counts or megakaryopoiesis.<sup>37</sup> (J.C.K., unpublished data) We also tested the effects of Frax1036, a specific small-molecule inhibitor of group I Paks.<sup>33</sup> Unlike the genetic deletion of *Pak2*, mice treated daily with Frax1036 for 3 weeks did not develop thrombocytopenia, nor other changes in peripheral blood (data not shown). Assuming effective inhibition of Pak2 kinase activity, these

results suggest that Pak2, similar to Pak1, may have kinase-independent functions that affect certain aspects of hematopoiesis in vivo.<sup>38-40</sup>

### Pak2 regulates megakaryocyte maturation

Mice with megakaryocyte-specific deletion of Pak-activating proteins, *Rac1/Cdc42*, are macrothrombocytopenic, with ultrastructurally abnormal megakaryocytes that fail to form proplatelets with defects in microtubule stabilization.<sup>25</sup> As Paks are downstream effectors of these GTPases, we sought to determine whether Pak activation is required for megakaryocyte development and function, as well as to maintain platelet counts.<sup>23-25</sup> As *Pak1*<sup>-/-</sup> mice do not have a notable platelet or megakaryocyte phenotype,<sup>37</sup> we examined the effects of genetic deletion of *Pak2* on megakaryocyte differentiation. We evaluated bone marrow for megakaryocyte number and morphology. Bone marrow from *Pak2*<sup>-/-</sup> mice had an increased number of mature megakaryocytes (CD41<sup>+</sup>) with increased diameter (Figure 1B-D).

We next sought to determine whether Pak kinase activity changed during stem cell maturation into megakaryocytes. We isolated CD34<sup>+</sup> stem cells and cultured them with TPO for 5 days. Sample lysates were collected and analyzed for activated Pak1/2/3, total Pak2, and CD41 protein expression (Figure 1E). Our results demonstrated that Pak1/2/3 activation increased during the maturation process, until decreasing at

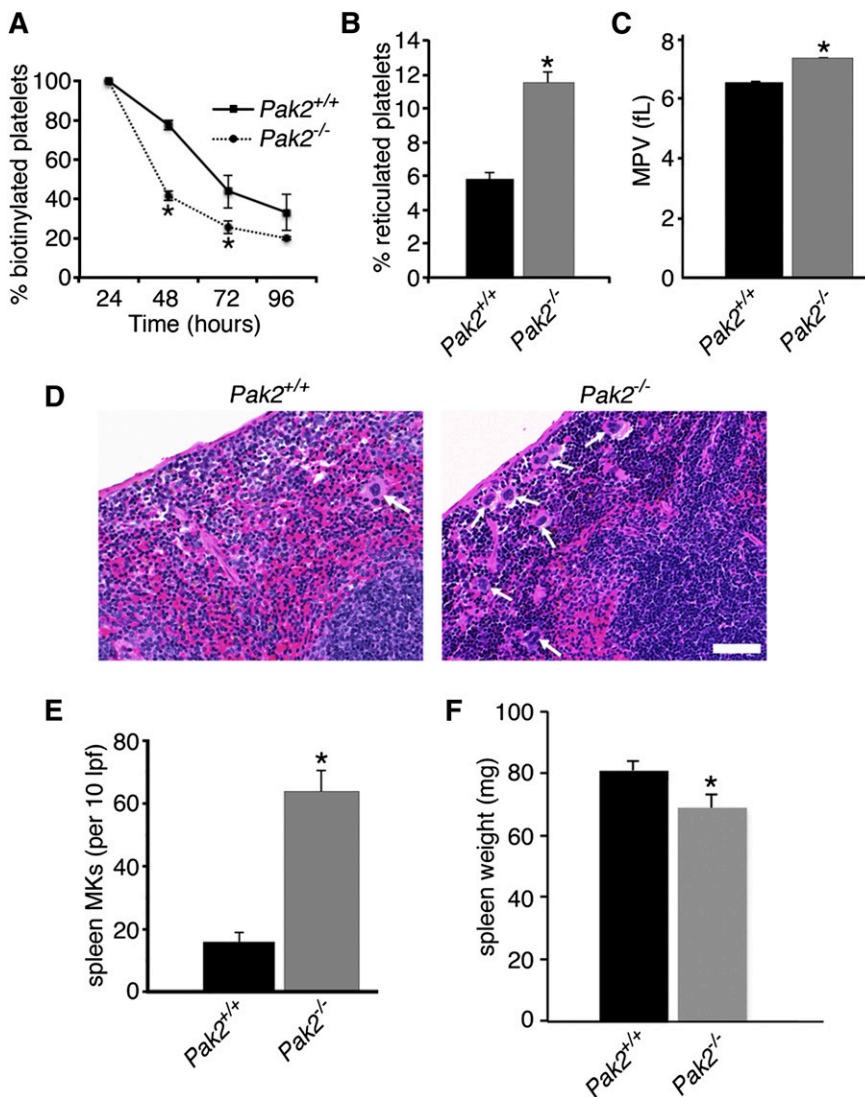
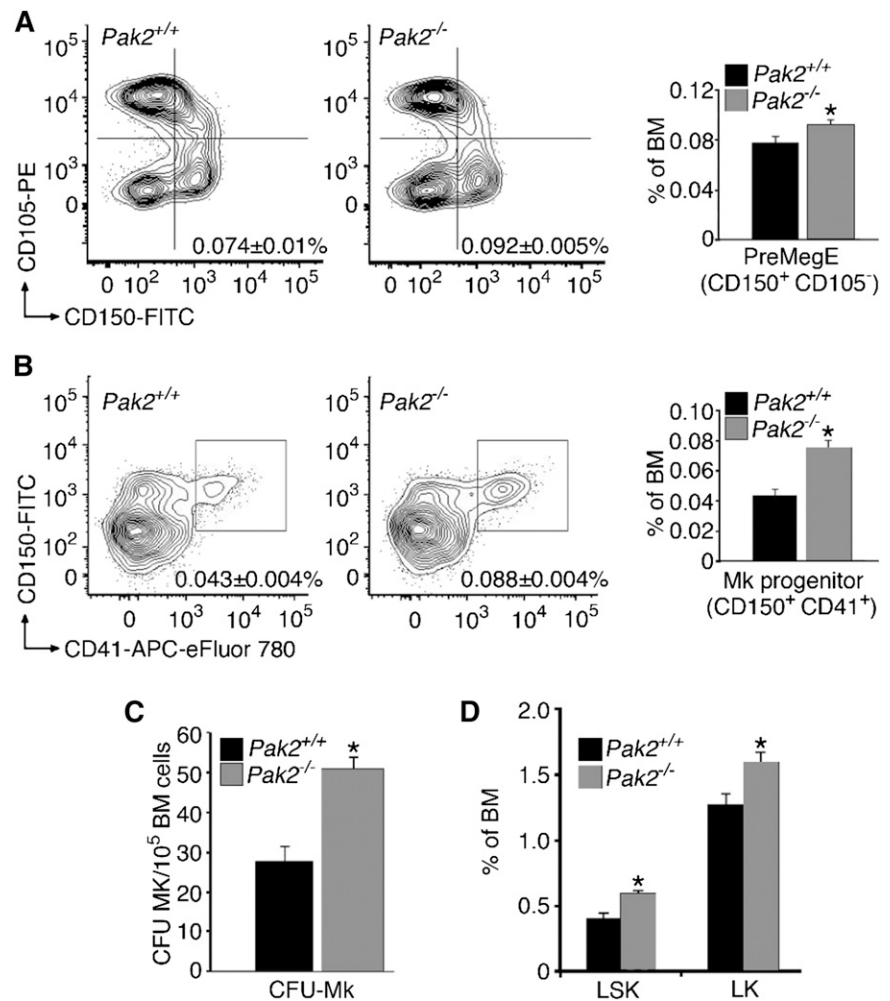


**Figure 2. Clearance rate and production of platelets is increased in Pak2-null mice.** (A) Quantification of in vivo biotinylated platelets 24, 48, 72, and 96 hours after *N*-hydroxysulfosuccinimidobiotin-biotin injection. Data expressed as percentage of baseline (24 hours postinjection; *n* = 4-8 mice/genotype per time point; mean ± SEM). (B) Quantification of the percentage of new, reticulated platelets as a percentage of total platelets (*n* > 5; mean ± SEM), 10 DPI. (C) MPV of *Pak2*<sup>+/+</sup> and *Pak2*<sup>-/-</sup> platelets, 14 DPI. (D) Representative images of hematoxylin and eosin stained spleen sections from *Pak2*<sup>+/+</sup> and *Pak2*<sup>-/-</sup> mice 14 DPI. Arrows indicate splenic megakaryocytes. Scale bar = 50 μm (40× original magnification). (E) Quantification of megakaryocytes in spleen sections counted in 10 low-power fields. (F) Spleen weight (mg) 14 DPI. All data from at least 3 mice/genotype; mean ± SEM. \**P* < .05.

**Figure 3. Pak2 deficiency increases megakaryocyte precursors and hematopoietic stem cells.** (A) Percentage of bone marrow from wild-type or *Pak2*<sup>-/-</sup> mice that are PreMegE identified by CD150<sup>+</sup> and CD105<sup>-</sup> after gating for Lin<sup>-</sup>C-kit<sup>+</sup>Sca1<sup>-</sup> (\**P* < .05). (B) Percentage of bone marrow from wild-type or *Pak2*<sup>-/-</sup> mice that are committed MkPs, defined by CD41<sup>+</sup> and CD150<sup>+</sup>, after gating for Lin<sup>-</sup>C-kit<sup>+</sup>Sca1<sup>-</sup> (\**P* < .0001). (C) MegaCult-C colony-formation assays (CFU-Mk) of 10<sup>5</sup> unsorted bone marrow cells from wild-type and *Pak2*<sup>-/-</sup> mice 14 DPI. Number of megakaryocyte colony-forming units (CFU-Mk) were counted after staining with acetylcholinesterase (\**P* < .0002). (D) Hematopoietic stem cells in bone marrow of wild-type and *Pak2*<sup>-/-</sup> mice. LSK, Lin<sup>-</sup>/C-kit<sup>+</sup>/Sca1<sup>+</sup>; LK, Lin<sup>-</sup>/C-kit<sup>+</sup>/Sca1<sup>-</sup> (\**P* < .05). All bone marrow measured at 14 DPI. Experiments included *n* > 5 mice/genotype, mean ± SEM.



the fully mature state (D5). Pak2 was substantially autophosphorylated in CD34<sup>+</sup> stem cells (D0), but this level, similar to that of pPak1/3, also increased during maturation (Figure 1E, top panel, lower band).

Localization and expression of Pak2 in mature megakaryocytes, proplatelets, and platelets was found throughout the maturation process (Figure 1F). Together, these data demonstrate that Pak2 has a role in megakaryocyte development from the stem cell to megakaryocyte.

#### **Pak2 deficiency increases platelet clearance rate and thrombopoiesis**

The combination of increased bone marrow megakaryocyte size and number, along with decreased platelet counts, suggests that *Pak2*<sup>-/-</sup> mice produce abnormal platelets with decreased survival in the circulation. To test whether platelet clearance was altered, we measured platelet life span, as well as the production of newly synthesized platelets.<sup>34</sup> *Pak2*<sup>-/-</sup> platelet life span was significantly reduced relative to wild-type mice (Figure 2A). These data are comparable to the shortened platelet life span in the *Rac1/Cdc42*<sup>-/-</sup> mice.<sup>25</sup> To assess whether platelet production was altered, we labeled blood samples ex vivo with thiazole orange.<sup>41</sup> As shown in Figure 2B, there was nearly double the amount of reticulated platelets in *Pak2*<sup>-/-</sup> mice compared with controls (wild-type, 5.8 ± 0.4% vs *Pak2*<sup>-/-</sup>, 11.5 ± 0.6%; mean ± standard error of the mean [SEM]) at 10 DPI. Young reticulated platelets are larger than older, nonreticulated platelets<sup>42,43</sup>; therefore, we evaluated MPV, and it was significantly increased in *Pak2*<sup>-/-</sup> mice (Figure 2C).

The spleen acts as a site for platelet clearance and production after bone marrow damage. Therefore, we evaluated the spleen for extramedullary megakaryopoiesis and discovered that *Pak2*<sup>-/-</sup> null spleens had significantly increased mature megakaryocytes; however, overall spleen weight was only slightly decreased (wild-type, 81 ± 3.5 mg; *Pak2*<sup>-/-</sup>, 70 ± 4 mg) (Figure 2D-F). Similar to bone marrow megakaryocytes, splenic megakaryocytes were also increased in diameter (supplemental Figure 1A, available on the *Blood* Web site). Increased platelet clearance can result in splenomegaly; however, our results demonstrated decreased spleen weight. Histological evaluation of *Pak2*<sup>-/-</sup> spleens demonstrated a distortion in normal splenic architecture, demonstrated by reduced white pulp, indicative of decreased lymphocytes and increased hemosiderin deposition (supplemental Figure 1B). Platelet clearance could still be occurring in the spleen, but other alterations to the spleen on Pak2 deletion make splenomegaly difficult to observe. Together, these data demonstrate that *Pak2*<sup>-/-</sup> mice are macrothrombocytopenic as a result of decreased platelet life span.

#### **Megakaryocyte progenitors are increased in Pak2-deficient mice**

Extensive flow cytometry studies have identified surface markers that constitute bone marrow megakaryocyte progenitors.<sup>36</sup> Because we observed significantly more mature megakaryocytes in *Pak2*<sup>-/-</sup> bone marrow (Figure 1D), we investigated whether there were also increased

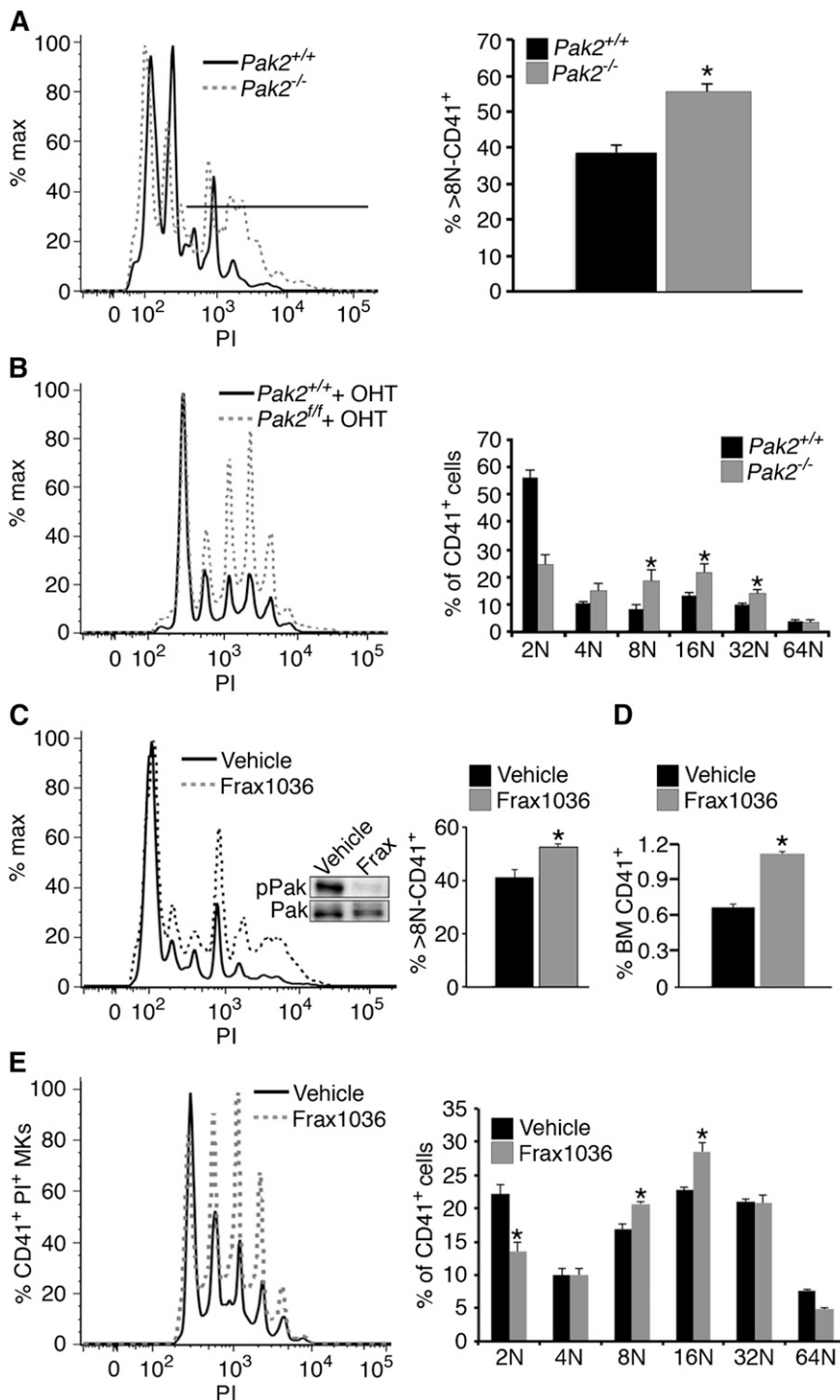


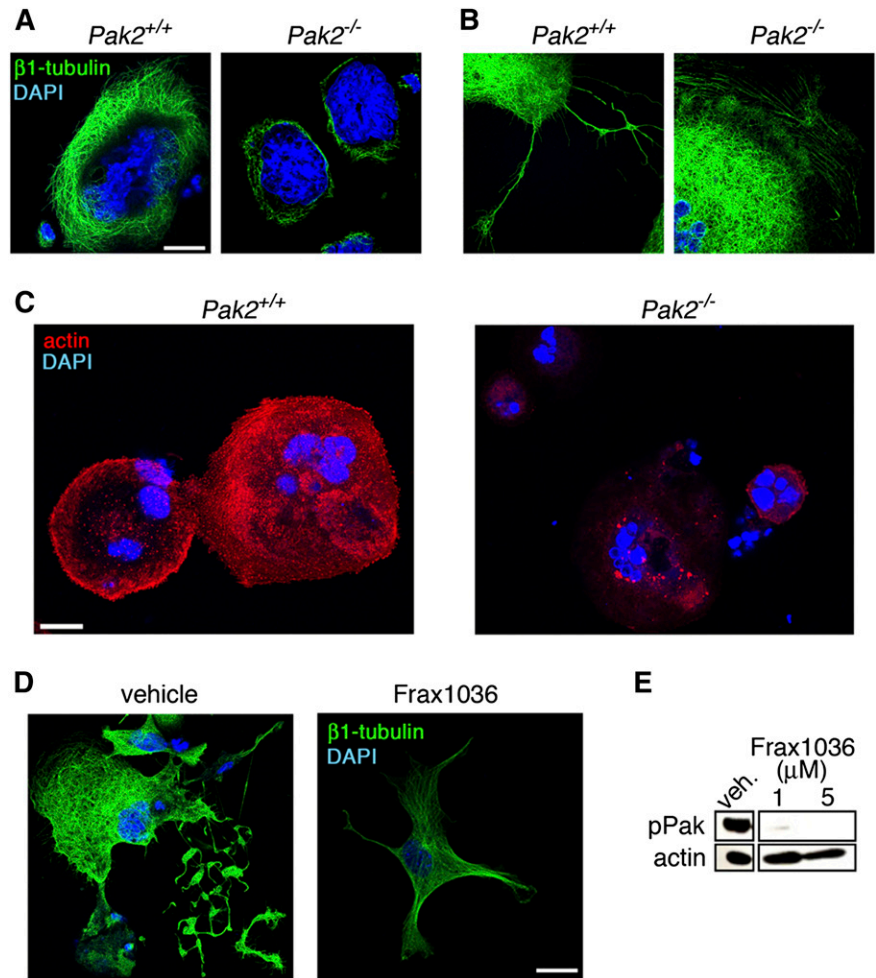
**Figure 4. *Pak2* is a negative regulator of megakaryocyte endomitosis.** (A) Megakaryocyte DNA content in wild-type and *Pak2*<sup>-/-</sup> mouse bone marrow, 14 DPI, was measured in CD41<sup>+</sup> bone marrow cells by flow cytometry. Line indicates location of 8N<sup>+</sup> cells ( $n > 10$ ; mean  $\pm$  SEM; \* $P < .05$ ). (B) Megakaryocyte DNA content in wild-type and *Pak2*<sup>-/-</sup> in vitro-derived megakaryocytes. Bone marrow cultured for 5 days with TPO and 500 nM 4-hydroxytamoxifen to activate *Cag-Cre-ERT2;Pak2*<sup>fl/fl</sup> transgene ( $n > 4$ , mean  $\pm$  SEM; \* $P < .05$ ). (C) Megakaryocyte DNA content in vehicle and Frax1036-treated mice. Mice were dosed with Frax1036 (Frax) ablates Pak1/2/3 Serine 141 phosphorylation (pPak) in the bone marrow relative to total Pak1/2/3 (Pak) (WB inset). Percentage greater than 8N DNA content, mean  $\pm$  SEM; \* $P < .05$ . (D) Percentage of CD41<sup>+</sup> bone marrow cells with Frax1036 treatment. Four mice/genotype, mean  $\pm$  SEM; \* $P < .001$ . (E) Bone marrow-derived megakaryocytes cultured with 0.5  $\mu$ M Frax1036 for 5 days;  $n > 5$  mice. 8N and 16N populations significantly increased in Frax1036-treated bone marrow ( $P < .008$  and  $P < .003$ , respectively).

megakaryocyte progenitors. The gating scheme used is delineated in supplemental Figure 2A. PreMegE cells are the progenitor cells that produce megakaryocytes and erythrocytes and have the highest capacity to form megakaryocyte colonies in vitro.<sup>36</sup> This population is defined as Lin<sup>-</sup>c-Kit<sup>+</sup>Sca1<sup>-</sup>CD41<sup>-</sup>Fc $\gamma$ R1/III<sup>-</sup>CD150<sup>+</sup>CD105<sup>-</sup>. We found that *Pak2*<sup>-/-</sup> bone marrow had significantly more bipotential PreMegE cells than wild-type bone marrow (Figure 3A). We next examined committed megakaryocyte progenitors (MkP) by expression of CD41 after gating for Lin<sup>-</sup>c-Kit<sup>+</sup>Sca1<sup>-</sup>CD150<sup>+</sup>. These progenitor cells represent an intermediate stage between the bipotential precursor

and mature megakaryocyte. Lineage-committed MkPs were significantly increased in the *Pak2*<sup>-/-</sup> bone marrow (Figure 3B).

Given the increase in megakaryocyte stem cell progenitors, we next tested whether these progenitors produced more mature megakaryocyte colonies. To address this question, we cultured an equal amount of unsorted bone marrow from wild-type and *Mx1cre*<sup>+</sup>*Pak2*<sup>fl/fl</sup> animals, 14 DPI injection, in a megakaryocyte specific colony-formation assay (CFU-MK). Analysis of the colonies with acetylcholinesterase staining after 8 to 10 days of growth with TPO, IL-3, and IL-6 demonstrated an increased number of colonies in *Pak2*<sup>-/-</sup> bone marrow, relative to

**Figure 5. Altered cytoskeleton structure in *Pak2*-null megakaryocytes.** (A) Analysis of  $\beta$ 1-tubulin structure and (B) proplatelet structure by fluorescence microscopy of wild-type and *Pak2*<sup>-/-</sup> megakaryocytes adhered to fibrinogen for 5 hours. Bone marrow treated with 500 nM 4-hydroxytamoxifen to induce *Cag-Cre-ERT2* expression and delete *Pak2*<sup>f/fi</sup>. Representative image of  $\beta$ 1-tubulin (green) and DAPI nuclear (blue) staining from 3 mice per genotype. (C) Representative Alexa Fluor 594-phalloidin staining for actin (red) and DAPI (blue) analyzed by fluorescence microscopy of wild-type and *Pak2*<sup>-/-</sup> megakaryocytes adhered to collagen for 5 hours. (D) Fetal liver-derived megakaryocytes treated with Frax1036 for duration of culture (4 days) and stained for  $\beta$ 1-tubulin (green) and DAPI (blue). (E) Western blot detection of serine 141 phosphorylated Pak1/2/3 (pPak) of fetal liver-derived megakaryocytes treated with Frax1036. Actin serves as a control for protein loading. Scale bar = 20  $\mu$ m for all images.



wild-type (Figure 3C). In addition, colony-forming potential on a per stem cell basis, examined by seeding equal number of sorted megakaryocyte precursors, was also increased in *Pak2*<sup>-/-</sup> bone marrow (supplemental Figure 2B). These results suggest that the number and proliferative potential of megakaryocyte progenitors are increased in *Pak2*-deficient mice.

Because *Pak2*<sup>-/-</sup> mice demonstrated altered megakaryopoiesis, we next asked whether loss of the *Pak2* gene was associated with abnormal hematopoiesis. Total bone marrow hematopoietic stem cells (LSK [*Lin*<sup>-</sup>/*C-kit*<sup>+</sup>/*Sca1*<sup>+</sup>]) and LK [*Lin*<sup>-</sup>/*C-kit*<sup>+</sup>/*Sca1*<sup>-</sup>]) were evaluated and significantly increased in *Pak2*<sup>-/-</sup> bone marrow (Figure 3D). LSK cells were further evaluated for number of long-term HSCs and multipotent progenitors, and both populations were increased (supplemental Figure 3A-B). Collectively, these findings identify *Pak2* as a negative regulator of megakaryocyte maturation via regulation of the bipotential precursors (PreMegE) and MkP cells in the bone marrow. The observed increase in megakaryocyte stem cells is not caused by elevated serum TPO levels induced by a reduction in circulating platelets (data not shown).

To examine whether expansion of megakaryocyte-erythroid progenitors also affected erythroid precursors, we examined bone marrow for erythroblasts (CD71<sup>hi</sup>Ter119<sup>hi</sup>) and erythrocytes (CD71<sup>lo</sup>Ter119<sup>hi</sup>) (supplemental Figure 4A-B). *Pak2* deletion significantly reduced early erythroblasts and increased mature erythrocytes in bone marrow. Ter119<sup>high</sup> cells were additionally analyzed for CD71 surface expression and size by FSC. *Pak2* deletion resulted in significant decreased

bone marrow immature and intermediate erythrocytes (EryA, EryB) and increased mature erythrocytes (EryC) (supplemental Figure 4C-D). Evaluation of erythroid stem cell progenitors (proerythroblasts), identified as *Lin*<sup>-</sup>/*C-kit*<sup>+</sup>/*Sca1*<sup>-</sup>/*CD41*<sup>-</sup>/*CD150*<sup>-</sup>/*CD105*<sup>+</sup>/*Ter119*<sup>+</sup>/*CD71*<sup>+</sup> was significantly decreased in *Pak2*-null bone marrow (supplemental Figure 4E). Together, these data demonstrate that *Pak2* deletion shifts the balance in the PreMegE stem cells toward the megakaryocyte lineage, leading to a decrease in expansion of proerythroblasts and erythroblasts.

#### Megakaryocyte endomitosis is negatively regulated by *Pak2*

Megakaryocytes progress through development to an endomitotic phase. Here cells are programmed to fail cytokinesis and accumulate DNA content in a single polylobulated nucleus before a final maturation state, consisting of proplatelet formation and platelet release.<sup>44,45</sup> Accordingly, we examined endomitosis (polyploidization) in megakaryocytes from *Pak2*<sup>-/-</sup> mice. We found that *Pak2* deletion in vivo markedly increased polyploidization of megakaryocytes (percentage of CD41<sup>+</sup> cells containing more than 8N DNA content) (Figure 4A). To determine whether this was cell-intrinsic, we measured polyploidy with in vitro-deleted megakaryocytes with tamoxifen-regulated Cre recombinase and found *Pak2* regulated polyploidization in a cell-intrinsic manner (Figure 4B). *Pak2*<sup>-/-</sup> megakaryocytes demonstrated significantly increased 8N, 16N, and 32N populations (*P* < .03). These in vitro data suggest that increased polyploidization observed in vivo is

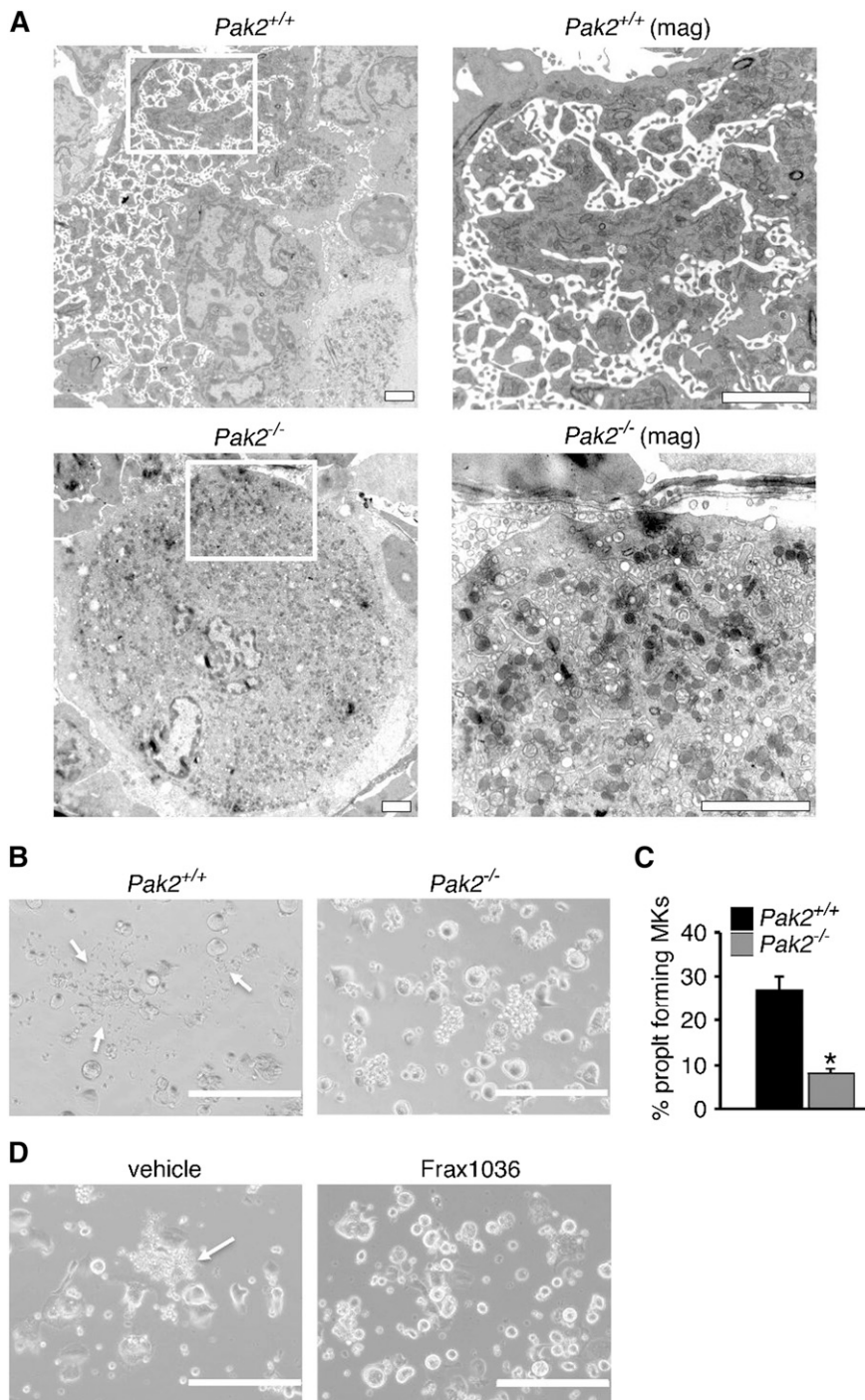


**Figure 6. Decreased proplatelets and altered ultrastructure of *Pak*-null megakaryocytes.** (A) Bone marrow imaged for megakaryocytes from wild-type and *Mx1cre<sup>+</sup>Pak2<sup>-/-</sup>* mice analyzed by transmission electron microscopy, 14 DPI. Wild-type megakaryocyte (upper, left,  $\times 5000$ ), periphery magnified (upper, right,  $\times 12000$ ). *Pak2<sup>-/-</sup>* megakaryocyte (lower, left,  $\times 5000$ ), periphery magnified (lower, right,  $\times 20000$ ). Scale bar = 2  $\mu\text{m}$ . (B) Proplatelet formation imaged from cultured megakaryocytes from wild-type and *Cag-Cre-ERT2<sup>+</sup>Pak2<sup>-/-</sup>* bone marrow, induced with 500 nM 4-hydroxytamoxifen and adhered to fibrinogen. White arrows indicate proplatelet. (C) Percentage proplatelet-forming megakaryocytes expressed as a percentage of total megakaryocytes per visual field  $\pm$  SEM,  $n = 5/\text{genotype}$ . Scale bar = 200  $\mu\text{m}$ . \* $P < .05$ . (D) Representative image of proplatelet formation in vehicle and Frax1036-treated bone marrow-derived megakaryocytes. Scale bar = 200  $\mu\text{m}$ . White arrows indicate proplatelet.

from cell-intrinsic signaling, but does not rule out influence from cell-extrinsic factors.

Small-molecule inhibitors specifically targeting group I Paks are currently being developed for the treatment of tumors overexpressing Pak proteins.<sup>10,28-30,46,47</sup> We examined whether treatment with group I-specific Pak inhibitor Frax1036 also altered megakaryocyte polyploidization or induced thrombocytopenia.<sup>33</sup> Treatment with Frax1036 for 3 weeks increased polyploidization in megakaryocytes and increased CD41<sup>+</sup> megakaryocytes (Figure 4C-D). Frax1036 treatment effectively ablated *Pak1-3* phosphorylation in the bone marrow (Figure 4C, inset). Bone marrow-derived megakaryocytes treated with Frax1036 also increased polyploidization at 8N and 16N ploidy stages

( $P < .008$  and  $P < .003$ , respectively) (Figure 4E). Collectively, these findings indicate that genetic deletion of *Pak2*, as well as pharmacologic kinase inhibition, causes increased megakaryocyte polyploidization in vivo and in vitro.

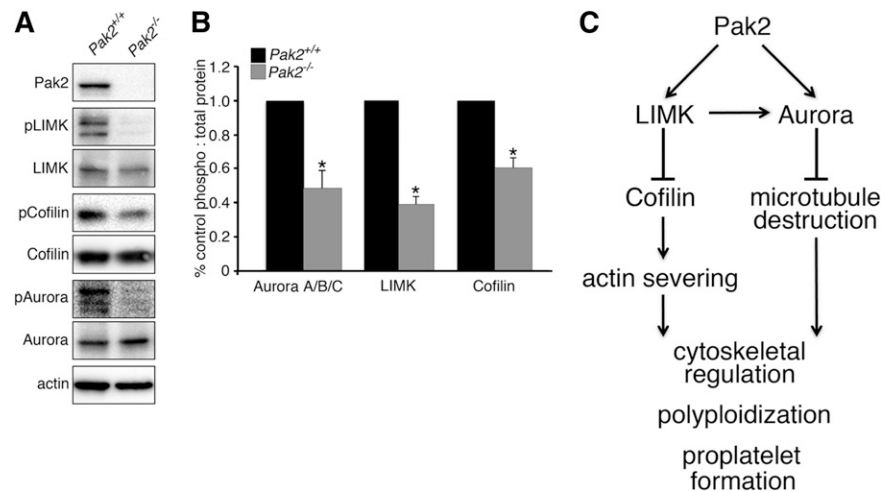
#### Altered cytoskeleton and ultrastructure of *Pak2<sup>-/-</sup>* megakaryocytes

During maturation, megakaryocytes undergo cytoskeletal alterations critical for polyploidization and proplatelet formation.<sup>48-50</sup> As Pak kinases are principally known for their regulation of actin and tubulin cytoskeleton networks,<sup>51</sup> we next measured  $\beta 1$ -tubulin expression in



**Figure 7. Altered phosphorylation of cytoskeleton regulatory proteins in *Pak2*-null megakaryocytes.**

(A) Western blot analysis of phosphorylation levels of cytoskeletal regulatory proteins LIMK, cofilin, and Aurora A/B/C in in vitro-deleted bone marrow-derived megakaryocytes (*CAG-Cre-ERT2<sup>+</sup>; Pak2<sup>-/-</sup>*). Equal quantities of total cellular protein were loaded and phospho-protein content was detected with phospho-specific antibodies (pLIMK, pCofilin, and pAurora) and total protein antibodies. Actin served as a control for equal loading. Blots are representative of at least 4 independent experiments. (B) Band densities quantified as a ratio of phospho:total protein and calculated as percentage of control. Densitometry was quantified with Fiji-Image J Software (National Institutes of Health). \**P* < .01. (C) Model depicting Pak2 regulation of megakaryocyte polyploidization and proplatelet formation through control of actin and microtubule networks.



megakaryocytes adherent to fibrinogen, relative to cell area. Quantitative fluorescence microscopy analyses found that *Pak2<sup>-/-</sup>* megakaryocytes expressed significantly less  $\beta$ 1-tubulin ( $24.1 \pm 2.5\%$ ) relative to wild-type megakaryocytes (Figure 5A). Proplatelet extension structures were also altered in *Pak2<sup>-/-</sup>* megakaryocytes (Figure 5B). Actin polymerization of megakaryocytes adherent to collagen was also decreased with *Pak2* deletion ( $57.6\% \pm 15.3\%$  decrease compared with wild-type) (Figure 5C). Similar to *Pak2<sup>-/-</sup>* megakaryocytes,  $\beta$ 1-tubulin staining decreased in Frax1036 treated-megakaryocytes, further supporting a role for Pak2 activity in megakaryocyte maturation and proplatelet formation (Figure 5D-E).

To better investigate megakaryocyte morphology in situ, we next examined wild-type and *Pak2<sup>-/-</sup>* bone marrow sections by transmission electron microscopy. Mature wild-type megakaryocytes displayed characteristic membrane invaginations, indicative of the invaginated membrane system (Figure 6A, top). *Pak2<sup>-/-</sup>* megakaryocytes demonstrated fewer invaginations in the periphery and around the nucleus (Figure 6A, bottom), supporting a role for Pak2 in proplatelet formation. Indeed, on adherence to fibrinogen, *Pak2<sup>-/-</sup>* bone marrow-derived megakaryocytes developed significantly fewer proplatelet extensions (Figure 6B-C). Consistent with genetic deletion, Frax1036-treated bone-marrow-derived megakaryocytes phenocopied *Pak2*-null megakaryocytes, with no proplatelet extensions observed (Figure 6D). Together, these data support a role for Pak2 in megakaryocyte cytoskeletal dynamics and ultrastructural mechanics that orchestrate proplatelet formation.

#### Altered signal transduction in *Pak2<sup>-/-</sup>* megakaryocytes

To establish a potential mechanism underlying the effects of *Pak2* deletion on megakaryocyte function, we next investigated the phosphorylation status of Pak2 effectors known to regulate cytoskeletal dynamics. We found that LIMK phosphorylation was significantly reduced (>60% reduction) and was associated with reduced phosphorylation of cofilin (>40% reduction) (Figure 7A-B) in *Pak2<sup>-/-</sup>* megakaryocytes. As cofilin is active in the nonphosphorylated state, these results suggest that *Pak2<sup>-/-</sup>* megakaryocytes undergo more rapid actin severing and depolymerization compared with wild-type megakaryocytes. Such properties have previously been associated with enhanced polyploidization in megakaryocytes.<sup>50,52</sup>

Similar to actin severing, enhanced microtubule depolymerization with colchicine, nocodazole, and vincristine have also been shown to enhance megakaryocyte ploidy.<sup>50,53,54</sup> Microtubule dynamics are regulated by a variety of proteins, including the Pak substrate Aurora

A,<sup>14,55</sup> a negative regulator of megakaryocyte polyploidization.<sup>56</sup> We evaluated *Pak2<sup>-/-</sup>* megakaryocytes for Aurora A/B/C phosphorylation and found markedly decreased levels in *Pak2<sup>-/-</sup>* cells compared with wild-type levels (>48% reduction) (Figure 7A-B). These data strongly suggest that Pak2 regulates multiple functions in the developing megakaryocyte by regulating both the actin and microtubule networks (Figure 7C).

## Discussion

Here we report a novel role for Pak2 in megakaryocyte biogenesis, cytoskeletal remodeling, proplatelet formation, and endomitosis. Using a conditional knockout mouse model, as well as a small-molecule inhibitor of group I Paks, we establish *Pak2* as regulator of the megakaryocyte cytoskeleton. We demonstrate that *Mxl1-cre<sup>Tg</sup>Pak2<sup>-/-</sup>* mice develop macrothrombocytopenia, which manifests in vivo with decreased platelet lifespan, along with increased mature megakaryocytes in the bone marrow and spleen, increased level of megakaryocyte ploidy, and increased megakaryocyte bone marrow progenitor cells. Pak2 also regulates megakaryocyte cytoskeleton structure, demonstrated with transmission electron microscopy of in situ bone marrow and immunofluorescence of in vitro primary culture of megakaryocytes.

Evidence from signaling studies suggests that at least 2 signaling pathways that regulate cytoskeletal function in megakaryocytes are regulated by Pak2: Aurora A, which classically regulates microtubule dynamics and mitotic entry; and LIMK/cofilin, which regulate actin dynamics (Figure 7). Aurora A deletion increases megakaryocyte differentiation and levels of polyploidization.<sup>56</sup> Aurora A could function to regulate polyploidization through its role in microtubule-organizing center localization, bipolar spindle formation, and inhibition of proteins that destabilize the microtubule network (ie, stathmin and mitotic centromere-associated kinesin).<sup>56-61</sup> We evaluated the effect of *Pak2* deletion on megakaryocyte Aurora activation and found that *Pak2<sup>-/-</sup>* megakaryocytes had decreased Aurora phosphorylation. Actin regulatory mechanisms mediated by the Pak effector LIMK and its substrate cofilin also play a role in later steps of megakaryocyte development, and in particular in proplatelet formation.<sup>62</sup> We observed significantly decreased F-actin formation in *Pak2*-null megakaryocytes (Figure 5C), supporting the hypothesis that *Pak2* deletion increases actin-severing activity of cofilin through LIMK inhibition. Notably, LIMK can also

directly phosphorylate Aurora to stabilize the microtubule network.<sup>63,64</sup> Thus, loss of LIMK phosphorylation in *Pak2*<sup>-/-</sup> megakaryocytes may serve to disrupt a signaling node between actin and microtubule systems, affecting both Aurora and cofilin activity (Figure 7C). However, LIMK regulation downstream of Pak is complex, as megakaryocyte double-knockout deletions of genes encoding the Pak activating proteins *Rac1/Cdc42* increase LIMK and cofilin phosphorylation.<sup>25</sup> Such findings support roles for *Rac1* and *Cdc42* beyond that of their effector *Pak2* alone and suggest that *Pak2* has a specific role in megakaryocyte endomitosis and proplatelet formation by means of regulating signal transduction cascades involved in cytoskeletal network regulation.

Although the use of the inducible Mx1-cre system for *Pak2* deletion in mice makes it difficult to determine whether our observations regarding megakaryocyte morphology, function, and platelet half-life are cell autonomous, our findings with *in vitro* megakaryocyte culture strongly suggest a cell-autonomous effect. *In vivo* bone marrow megakaryocyte ultrastructure revealed disrupted megakaryocyte plasma membrane invaginations (Figure 6A) in the Mx1-cre model system. Consistent with *in vivo* data, *in vitro* megakaryocytes were also defective in their structure, mainly observed by defects in proplatelet formation, using both a genetic and pharmacological model (Figure 6B-C). Elevated levels of polyploidization were also observed both *in vivo* and *in vitro* (Figure 4). These data strongly suggest a cell-autonomous role for *Pak2* in megakaryocytes. It remains possible, however, that there are also non-cell-autonomous effects related to *Pak2* deletion in other hematopoietic lineages in Mx1-cre mice, especially given the known role of *Pak2* in hematopoietic stem cells and their progeny.<sup>15,32,65</sup> These issues will be addressed in future studies using transgenic mice with megakaryocyte-specific Cre drivers such as PF4-cre.<sup>66</sup>

In summary, our results demonstrate that *Pak2* regulates megakaryocytes, in part through signaling networks that regulate actin and microtubule cytoskeleton. This multiregulatory influence of *Pak2*, through phosphorylation of LIMK and Aurora, supports a role for *Pak2* in controlling the dynamic cytoskeleton of developing megakaryocytes to play a novel role in megakaryocyte biology.

## Acknowledgments

We thank J. Oesterling (Fox Chase Cancer Center Flow Cytometry Core) for flow cytometry assistance, A. Efimov (Fox Chase Cancer Center Microscopy Core), and D. Williams (University of Pennsylvania, Electron Microscopy Resource Laboratory) for imaging assistance. We also thank Dr J. Field, Dr S. Ryeom, Dr S. Sykes, Dr A. Mazharian, and Dr M. Larson for insightful comments.

This work was supported by grants from the National Institutes of Health, National Cancer Institute (R01-CA142928 and R01-CA148805 to J.C., and F31-CA177182 to R.E.K.), the Fox Chase Cancer Center (P30-CA006927), the National Heart, Lung, and Blood Institute (R01-HL101972 to O.J.T.M.; and R01-HL118593 and R01-HL93231 to A.P.K.), as well as by an appropriation from the State of Pennsylvania. In addition, grant funding was provided from the American Heart Association (13POST13730003 to J.E.A.; 15POST22420000 to J.C.K.; and 13EIA12630000 to O.J.T.M.).

## Authorship

Contribution: R.E.K., J.E.A., O.J.T.M., and J.C. conception and design of research; R.E.K., J.E.A., J.C.K., H.Y.C., T.Y.P., and O.J.T.M. performed experiments; E.D. performed pathology; R.E.K., J.E.A., O.J.T.M. and J.C. analyzed data; R.E.K., J.E.A., E.D., O.J.T.M., and J.C. interpreted results of experiments; R.E.K. and J.E.A. prepared figures; R.E.K., J.E.A., O.J.T.M., and J.C. drafted the manuscript; R.E.K., J.E.A., O.J.T.M., and J.C. edited and revised the manuscript; and R.E.K., J.E.A., J.C.K., E.D., H.Y.C., T.Y.P., M.R., S.P.K., O.J.T.M., and J.C. approved the final version of manuscript.

Conflict-of-interest disclosure: The authors declare no competing financial interests.

Correspondence: Jonathan Chernoff, 333 Cottman Ave, W451, Philadelphia, PA 19111; e-mail: j\_chernoff@fccc.edu.

## References

- Nakeff A, Maat B. Separation of megakaryocytes from mouse bone marrow by velocity sedimentation. *Blood*. 1974;43(4):591-595.
- Avraham H. Regulation of megakaryocytopoiesis. *Stem Cells*. 1993;11(6):499-510.
- Thon JN, Montalvo A, Patel-Hett S, et al. Cytoskeletal mechanics of proplatelet maturation and platelet release. *J Cell Biol*. 2010;191(4):861-874.
- Machlus KR, Italiano JE Jr. The incredible journey: From megakaryocyte development to platelet formation. *J Cell Biol*. 2013;201(6):785-796.
- Thon JN, Mazutis L, Wu S, et al. Platelet bioreactor-on-a-chip. *Blood*. 2014;124(12):1857-1867.
- de Sauvage FJ, Hass PE, Spencer SD, et al. Stimulation of megakaryocytopoiesis and thrombopoiesis by the c-Mpl ligand. *Nature*. 1994;369(6481):533-538.
- Mazharian A, Watson SP, Severin S. Critical role for ERK1/2 in bone marrow and fetal liver-derived primary megakaryocyte differentiation, motility, and proplatelet formation. *Exp Hematol*. 2009;37(10):1238-1249.
- Rojnuckarin P, Drachman JG, Kaushansky K. Thrombopoietin-induced activation of the mitogen-activated protein kinase (MAPK) pathway in normal megakaryocytes: role in endomitosis. *Blood*. 1999;94(4):1273-1282.
- Nakao T, Geddis AE, Fox NE, Kaushansky K. PI3K/Akt/FOXO3a pathway contributes to thrombopoietin-induced proliferation of primary megakaryocytes *in vitro* and *in vivo* via modulation of p27(Kip1). *Cell Cycle*. 2008;7(2):257-266.
- Radu M, Semenova G, Kosoff R, Chernoff J. PAK signalling during the development and progression of cancer. *Nat Rev Cancer*. 2014;14(1):13-25.
- Coles LC, Shaw PE. PAK1 primes MEK1 for phosphorylation by Raf-1 kinase during cross-cascade activation of the ERK pathway. *Oncogene*. 2002;21(14):2236-2244.
- Edwards DC, Sanders LC, Bokoch GM, Gill GN. Activation of LIM-kinase by Pak1 couples Rac/Cdc42 GTPase signalling to actin cytoskeletal dynamics. *Nat Cell Biol*. 1999;1(5):253-259.
- Kosoff R, Chow HY, Radu M, Chernoff J. Pak2 kinase restrains mast cell FcεR1 receptor signaling through modulation of Rho protein guanine nucleotide exchange factor (GEF) activity. *J Biol Chem*. 2013;288(2):974-983.
- Zhao ZS, Lim JP, Ng YW, Lim L, Manser E. The GIT-associated kinase PAK targets to the centrosome and regulates Aurora-A. *Mol Cell*. 2005;20(2):237-249.
- Dorrance AM, De Vita S, Radu M, et al. The Rac GTPase effector p21-activated kinase is essential for hematopoietic stem/progenitor cell migration and engraftment. *Blood*. 2013;121(13):2474-2482.
- Arai A, Jin A, Yan W, et al. SDF-1 synergistically enhances IL-3-induced activation of the Raf-1/MEK/Erk signaling pathway through activation of Rac and its effector Pak kinases to promote hematopoiesis and chemotaxis. *Cell Signal*. 2005;17(4):497-506.
- Aslan JE, Baker SM, Loren CP, et al. The PAK system links Rho GTPase signaling to thrombin-mediated platelet activation. *Am J Physiol Cell Physiol*. 2013;305(5):C519-C528.
- Aslan JE, Itakura A, Haley KM, et al. p21 activated kinase signaling coordinates glycoprotein receptor VI-mediated platelet aggregation, lamellipodia formation, and aggregate stability under shear. *Arterioscler Thromb Vasc Biol*. 2013;33(7):1544-1551.
- Crespin M, Vidal C, Picard F, Lacombe C, Fontenay M. Activation of PAK1/2 during the shedding of platelet microvesicles. *Blood Coagul Fibrinolysis*. 2009;20(1):63-70.
- Suzuki-Inoue K, Yatomi Y, Asazuma N, et al. Rac, a small guanosine triphosphate-binding protein, and p21-activated kinase are activated during platelet spreading on collagen-coated surfaces:

- roles of integrin alpha(2)beta(1). *Blood*. 2001; 98(13):3708-3716.
21. Vidal C, Geny B, Melle J, Jandrot-Perrus M, Fontenay-Roupey M. Cdc42/Rac1-dependent activation of the p21-activated kinase (PAK) regulates human platelet lamellipodia spreading: implication of the cortical-actin binding protein cortactin. *Blood*. 2002;100(13):4462-4469.
  22. Teo M, Manser E, Lim L. Identification and molecular cloning of a p21cdc42/rac1-activated serine/threonine kinase that is rapidly activated by thrombin in platelets. *J Biol Chem*. 1995;270(44):26690-26697.
  23. Akbar H, Kim J, Funk K, et al. Genetic and pharmacologic evidence that Rac1 GTPase is involved in regulation of platelet secretion and aggregation. *J Thromb Haemost*. 2007;5(8):1747-1755.
  24. Akbar H, Shang X, Perveen R, et al. Gene targeting implicates Cdc42 GTPase in GPVI and non-GPVI mediated platelet filopodia formation, secretion and aggregation. *PLoS ONE*. 2011;6(7):e22117.
  25. Pleines I, Dütting S, Cherpokova D, et al. Defective tubulin organization and proplatelet formation in murine megakaryocytes lacking Rac1 and Cdc42. *Blood*. 2013;122(18):3178-3187.
  26. Menges CW, Sementino E, Talarchek J, et al. Group I p21-activated kinases (PAKs) promote tumor cell proliferation and survival through the AKT1 and Raf-MAPK pathways. *Mol Cancer Res*. 2012;10(9):1178-1188.
  27. Deacon SW, Beeser A, Fukui JA, et al. An isoform-selective, small-molecule inhibitor targets the autoregulatory mechanism of p21-activated kinase. *Chem Biol*. 2008;15(4):322-331.
  28. Licciulli S, Maksimoska J, Zhou C, et al. FRAX597, a small molecule inhibitor of the p21-activated kinases, inhibits tumorigenesis of neurofibromatosis type 2 (NF2)-associated Schwannomas. *J Biol Chem*. 2013;288(40):29105-29114.
  29. Ong CC, Jubb AM, Jakubiak D, et al. P21-activated kinase 1 (PAK1) as a therapeutic target in BRAF wild-type melanoma. *J Natl Cancer Inst*. 2013;105(9):606-607.
  30. Crawford JJ, Hoeflich KP, Rudolph J. p21-Activated kinase inhibitors: a patent review. *Expert Opin Ther Pat*. 2012;22(3):293-310.
  31. Kühn R, Schwenk F, Aguet M, Rajewsky K. Inducible gene targeting in mice. *Science*. 1995; 269(5229):1427-1429.
  32. Phee H, Au-Yeung BB, Pryshchep O, et al. Pak2 is required for actin cytoskeleton remodeling, TCR signaling, and normal thymocyte development and maturation. *eLife*. 2014;3:e02270.
  33. Chow HY, Dong B, Duron SG, et al. Group I Paks as therapeutic targets in NF2-deficient meningioma. *Oncotarget*. 2015;6(4):1981-1994.
  34. Prisolovsky A, Marathe B, Hosni A, et al. Rapid platelet turnover in WASP(-) mice correlates with increased ex vivo phagocytosis of opsonized WASP(-) platelets. *Exp Hematol*. 2008;36(5):609-623.
  35. Kostyak JC, Naik MU, Naik UP. Calcium- and integrin-binding protein 1 regulates megakaryocyte ploidy, adhesion, and migration. *Blood*. 2012;119(3):838-846.
  36. Pronk CJ, Rossi DJ, Månsson R, et al. Elucidation of the phenotypic, functional, and molecular topography of a myeloid progenitor cell hierarchy. *Cell Stem Cell*. 2007;1(4):428-442.
  37. Allen JD, Jaffer ZM, Park SJ, et al. p21-activated kinase regulates mast cell degranulation via effects on calcium mobilization and cytoskeletal dynamics. *Blood*. 2009;113(12):2695-2705.
  38. Higuchi M, Onishi K, Kikuchi C, Gotoh Y. Scaffolding function of PAK in the PDK1-Akt pathway. *Nat Cell Biol*. 2008;10(11):1356-1364.
  39. Staser K, Shew MA, Michels EG, et al. A Pak1-PP2A-ERM signaling axis mediates F-actin rearrangement and degranulation in mast cells. *Exp Hematol*. 2013;41(1):56-66.
  40. Badolia R, Manne BK, Dangelmaier C, Chernoff J, Kunapuli SP. Gq-mediated Akt translocation to the membrane: a novel PIP3-independent mechanism in platelets. *Blood*. 2015;125(1):175-184.
  41. Lee LG, Chen CH, Chiu LA. Thiazole orange: a new dye for reticulocyte analysis. *Cytometry*. 1986;7(6):508-517.
  42. Koh KR, Yamane T, Ohta K, Hino M, Takubo T, Tatum N. Pathophysiological significance of simultaneous measurement of reticulated platelets, large platelets and serum thrombopoietin in non-neoplastic thrombocytopenic disorders. *Eur J Haematol*. 1999;63(5):295-301.
  43. Guthikonda S, Alviar CL, Vaduganathan M, et al. Role of reticulated platelets and platelet size heterogeneity on platelet activity after dual antiplatelet therapy with aspirin and clopidogrel in patients with stable coronary artery disease. *J Am Coll Cardiol*. 2008;52(9):743-749.
  44. Ebbe S. Biology of megakaryocytes. *Prog Hemost Thromb*. 1976;3:211-229.
  45. Machlus KR, Thon JN, Italiano JE Jr. Interpreting the developmental dance of the megakaryocyte: a review of the cellular and molecular processes mediating platelet formation. *Br J Haematol*. 2014; 165(2):227-236.
  46. Chow HY, Jubb AM, Koch JN, et al. p21-Activated kinase 1 is required for efficient tumor formation and progression in a Ras-mediated skin cancer model. *Cancer Res*. 2012;72(22):5966-5975.
  47. Molli PR, Li DQ, Murray BW, Rayala SK, Kumar R. PAK signaling in oncogenesis. *Oncogene*. 2009;28(28):2545-2555.
  48. Patel SR, Richardson JL, Schulze H, et al. Differential roles of microtubule assembly and sliding in proplatelet formation by megakaryocytes. *Blood*. 2005;106(13):4076-4085.
  49. Patel-Hett S, Richardson JL, Schulze H, et al. Visualization of microtubule growth in living platelets reveals a dynamic marginal band with multiple microtubules. *Blood*. 2008;111(9):4605-4616.
  50. Tablin F, Castro M, Leven RM. Blood platelet formation in vitro. The role of the cytoskeleton in megakaryocyte fragmentation. *J Cell Sci*. 1990; 97(Pt 1):59-70.
  51. Zhao ZS, Manser E. PAK family kinases: Physiological roles and regulation. *Cell Logist*. 2012;2(2):59-68.
  52. Baatout S, Chatelain B, Staquet P, Symann M, Chatelain C. Inhibition of actin polymerization by cytochalasin B induces polyploidization and increases the number of nucleolar organizer regions in human megakaryocyte cell lines. *Anticancer Res*. 1998;18(1A):459-464.
  53. Baatout S, Chatelain B, Staquet P, Symann M, Chatelain C. Inhibition of tubulin polymerization in megakaryocyte cell lines leads to polyploidization which affects the metabolism of actin. *Anticancer Res*. 1998;18(3A):1553-1561.
  54. van der Loo B, Hong Y, Hancock V, Martin JF, Erusalimsky JD. Antimicrotubule agents induce polyploidization of human leukaemic cell lines with megakaryocytic features. *Eur J Clin Invest*. 1993; 23(10):621-629.
  55. Ando Y, Yasuda S, Ocegüera-Yanez F, Narumiya S. Inactivation of Rho GTPases with Clostridium difficile toxin B impairs centrosomal activation of Aurora-A in G2/M transition of HeLa cells. *Mol Biol Cell*. 2007;18(10):3752-3763.
  56. Wen Q, Goldenson B, Silver SJ, et al. Identification of regulators of polyploidization presents therapeutic targets for treatment of AMKL. *Cell*. 2012;150(3):575-589.
  57. Goldenson B, Kirsammer G, Stankiewicz MJ, Wen QJ, Crispino JD. Aurora kinase A is required for hematopoiesis, but is dispensable for murine megakaryocyte endomitosis and differentiation. *Blood*. 2015;(Feb):10.
  58. Avanzi MP, Chen A, He W, Mitchell WB. Optimizing megakaryocyte polyploidization by targeting multiple pathways of cytokinesis. *Transfusion*. 2012;52(11):2406-2413.
  59. Lordier L, Jalil A, Aurade F, et al. Megakaryocyte endomitosis is a failure of late cytokinesis related to defects in the contractile ring and Rho/Rock signaling. *Blood*. 2008;112(8):3164-3174.
  60. Lordier L, Chang Y, Jalil A, et al. Aurora B is dispensable for megakaryocyte polyploidization, but contributes to the endomitotic process. *Blood*. 2010;116(13):2345-2355.
  61. Geddis AE, Kaushansky K. Endomitotic megakaryocytes form a midzone in anaphase but have a deficiency in cleavage furrow formation. *Cell Cycle*. 2006;5(5):538-545.
  62. Bender M, Eckly A, Hartwig JH, et al. ADF/cofilin-dependent actin turnover determines platelet formation and sizing. *Blood*. 2010; 116(10):1767-1775.
  63. Petrilli A, Copik A, Posadas M, et al. LIM domain kinases as potential therapeutic targets for neurofibromatosis type 2. *Oncogene*. 2014; 33(27):3571-3582.
  64. Prudent R, Vassal-Stermann E, Nguyen CH, et al. Pharmacological inhibition of LIM kinase stabilizes microtubules and inhibits neoplastic growth. *Cancer Res*. 2012;72(17):4429-4439.
  65. Zeng Y, Broxmeyer HE, Staser K, et al. Pak2 regulates hematopoietic progenitor cell proliferation, survival and differentiation. *Stem Cells*. 2015;(Jan):13.
  66. Tiedt R, Schomber T, Hao-Shen H, Skoda RC. Pf4-Cre transgenic mice allow the generation of lineage-restricted gene knockouts for studying megakaryocyte and platelet function in vivo. *Blood*. 2007;109(4):1503-1506.